Dentomaxillofacial Radiology (2015) 44, 20150108

birpublications.org/dmfr

RESEARCH ARTICLE

Optimization of dental CBCT exposures through mAs reduction

[1,2]R Pauwels, [2]L Seynaeve, [2]J C G Henriques, [3]C de Oliveira-Santos, [4]P C Souza, [4]F H Westphalen, [5]I R F Rubira-Bullen, [6]R F Ribeiro-Rotta, [7]M I B Rockenbach, [8]F Haiter-Neto, [1,2]P Pittayapat, [9]H Bosmans, [10]R Bogaerts and [1]R Jacobs

[1]Department of Radiology, Faculty of Dentistry, Chulalongkorn University, Bangkok, Thailand; [2]OMFS-IMPATH Research Group, Oral Imaging Center, Department of Imaging and Pathology, Biomedical Sciences Group, University of Leuven, Leuven, Belgium; [3]Department of Stomatology, Public Health and Forensic Dentistry, University of São Paulo, School of Dentistry of Ribeirão Preto of Dentistry, São Paulo, Brazil; [4]School of Dentistry, Pontifical Catholic University of Paraná, Curitiba, Brazil; [5]Stomatology Department, Bauru School of Dentistry, University of São Paulo, São Paulo, Brazil; [6]Department of Oral Medicine, School of Dentistry, Federal University of Goiás, Goiás, Brazil; [7]Department of Surgery, Faculty of Dentistry, Pontifical Catholic University of Rio Grande do Sul, Porto Alegre, Rio Grande do Sul, Brazil; [8]Department of Oral Diagnosis, Piracicaba Dental School, University of Campinas, Piracicaba, Brazil; [9]Department of Radiology, University Hospitals Leuven, Leuven, Belgium; [10]Department of Experimental Radiotherapy, University Hospitals Leuven, Leuven, Belgium

Objectives: To investigate the effect of tube current–exposure time (mAs) reduction on clinical and technical image quality for different CBCT scanners, and to determine preliminary minimally acceptable values for the mAs and contrast-to-noise ratio (CNR) in CBCT.
Methods: A polymethyl methacrylate (PMMA) phantom and an anthropomorphic skull phantom, containing a human skeleton embedded in polyurethane, were scanned using four CBCT devices, including seven exposure protocols. For all protocols, the mAs was varied within the selectable range. Using the PMMA phantom, the CNR_{AIR} was measured and corrected for voxel size. Eight axial slices and one coronal slice showing various anatomical landmarks were selected for each CBCT scan of the skull phantom. The slices were presented to six dentomaxillofacial radiologists, providing scores for various anatomical and diagnostic parameters.
Results: A hyperbolic relationship was seen between CNR_{AIR} and mAs. Similarly, a gradual reduction in clinical image quality was seen at lower mAs values; however, for several protocols, image quality remained acceptable for a moderate or large mAs reduction compared with the standard exposure setting, depending on the clinical application. The relationship between mAs, CNR_{AIR} and observer scores was different for each CBCT device. Minimally acceptable values for mAs were between 9 and 70, depending on the criterion and clinical application.
Conclusions: Although noise increased at a lower mAs, clinical image quality often remained acceptable at exposure levels below the manufacturer's recommended setting, for certain patient groups. Currently, it is not possible to determine minimally acceptable values for image quality that are applicable to multiple CBCT models.
Dentomaxillofacial Radiology (2015) **44**, 20150108. doi: 10.1259/dmfr.20150108

Cite this article as: Pauwels R, Seynaeve L, Henriques JCG, de Oliveira-Santos C, Souza PC, Westphalen FH, et al. Optimization of dental CBCT exposures through mAs reduction. *Dentomaxillofac Radiol* 2015; **44**: 20150108.

Keywords: cone-beam computed tomography; computer-assisted radiographic image interpretation; computer-assisted image processing; quality control

Introduction

CBCT has become an indispensible imaging tool for a variety of dental applications. Although its use has lead to improved diagnosis and treatment planning for

Correspondence to: Dr Ruben Pauwels. E-mail: pauwelsruben@hotmail.com
Received 22 March 2015; revised 19 May 2015; accepted 18 June 2015

a wide array of patient groups, its widespread use has raised concerns regarding the risks related to its patient radiation dose.[1] Seeing that CBCT doses are considerably higher than those of intraoral, panoramic and cephalometric radiography, it is pivotal to consider all possibilities to reduce patient dose to the minimum level, according to the "as low as reasonably achievable" principle.[2]

In current practice, exposure settings in CBCT are initially determined by the manufacturer. Many CBCT models have pre-set exposure settings for patients of different sizes and/or for different clinical applications (*e.g.* "endodontic" or "implant" modes); others allow the user to freely select exposure parameters such as kV, mA and exposure time within a certain range.[3] While the use of "default" exposure settings will assure adequate image quality, the user should always consider the possibility of reducing the exposure at an individual patient level, depending on factors such as patient size and clinical indication. A recent study concluded that a reduction in tube current (mA) [or tube current–exposure time product (mAs)] is preferred over a kV reduction in dental CBCT, as it coincides with a smaller reduction in image quality at a given dose level.[4] Seeing that mAs is linearly related to patient dose, the user should select the lowest mAs level that results in an acceptable image quality.

The image quality of CBCT scanners has been extensively studied *in vitro* and *in vivo*. Most studies have focused on certain clinical image quality aspects, such as the visibility of anatomical landmarks, the detection of caries, bone loss or bony lesions, and the segmentation accuracy of teeth and bones.[5–9] Different skull and jaw models were used, which limits the standardization and intercomparison of quantitative image quality measurements. In addition, findings from these studies are often limited to the investigated type(s) of scanner owing to large difference in image quality between CBCT models.[10]

Alternatively, geometrical phantoms have been used to investigate technical image quality parameters.[11–14] For straightforward image quality parameters such as contrast, noise and the variability of grey values, using these types of phantoms allows for a reproduction of the measurements on any type of scanner. Furthermore, the use of a geometrical image quality phantom in quality control could lead to a standardization of the quality assurance of CBCT devices, and to the possible implementation of objective image quality criteria, which can guide the user or medical physicist in the evaluation of a scanner's performance.[15] The limitation of using technical image quality parameters as minimally acceptable values for clinical practice is that there is no straightforward way of translating these parameters to clinical image quality. In practice, the choice of exposure protocols for different patient groups is left to the subjective interpretation of the operator (*i.e.* dentist, radiologist, X-ray technician), seeing that there are no guidance levels for radiation dose or image quality. Whether or not an image is acceptable for clinical purposes is determined by the observer of the image, adding another degree of subjectivity to the use of CBCT.[16–19] Therefore, the use of objective image quality criteria could lead to improved strategies for optimization of exposures in CBCT.

The aim of this study was to investigate the effect of mAs reduction on the contrast-to-noise ratio (CNR) and clinical image quality for different CBCT scanners. An additional objective was to determine preliminary minimally acceptable values for mAs and CNR.

Methods and materials

CBCT devices

Four CBCT devices were included in this study: 3D Accuitomo® 170 (J. Morita Manufacturing Corporation, Kyoto, Japan), CRANEX® 3D and SCANORA® 3D (Soredex, Tuusula, Finland), and GALILEOS® Comfort (Sirona Dental Systems Gmbh, Bensheim, Germany). For these devices, a total of seven imaging protocols, determined by the field of view (FOV) size and voxel size, were selected (Table 1). For the 3D Accuitomo 170 and SCANORA 3D, a small and large FOV size with varying voxel size was selected. For the CRANEX 3D, a high- and low-resolution protocol was selected for the largest available FOV. For the Galileos Comfort, only one protocol was included, as the FOV and voxel size were fixed. The full available mAs range was used for each imaging protocol, resulting in a total of 47 exposure settings. For the 3D Accuitomo 170, the highest available mAs values (131–175 mAs) were used

Table 1 CBCT devices and exposure parameters

CBCT	*Field of view (cm)*	*Voxel size (mm)*	*kV*	*mAs range*	*Number of scans*
3D Accuitomo 170	14 × 10	0.25	90	17.5–123	7[a]
	6 × 6	0.125	90	17.5–123	7[a]
SCANORA 3D	13.5 × 14.5	0.35	90	9–29	6
	6 × 6	0.2	90	12–39	6
CRANEX 3D	6 × 8	0.2	90	51–126	5
	6 × 8	0.3	90	29–63	4
GALILEOS Comfort	15 × 15	0.29	85	10–42	5

kV, tube voltage; mAs, tube current–exposure time product.
CRANEX® 3D and SCANORA® 3D were obtained from Soredex, Tuusula, Finland, GALILEOS® Comfort was obtained from Sirona Dental Systems Gmbh, Bensheim, Germany and 3D Accuitomo® 170 was obtained from J. Morita Manufacturing Corporation, Kyoto, Japan.
[a]For the contrast/noise analysis, the mAs interval was halved and the maximum mAs was set at 175, resulting in a total of 19 scans.

for CNR measurements but not for clinical image quality evaluation, as they are up to 100% higher than the default clinical mAs settings for that device.

Technical image quality

A head-sized polymethyl methacrylate (PMMA) phantom (⌀16 cm) was used for the analysis of CNR. The phantom is homogeneous with the exception of a central air hole of ⌀10 mm at the bottom. As this air hole was needed for CNR measurements, the phantom was placed on another PMMA phantom, allowing for the bottom part to be scanned without interference from supporting structures (*e.g.* metal platforms).

All data sets were exported as axial slices in digital imaging and communications in medicine format and evaluated with ImageJ software v. 1.41 (National Institutes of Health, Bethesda, MD). All measurements were performed by two researchers and the values were averaged.

CNR was measured between the air hole and the PMMA by measuring the mean grey value and standard deviation for both materials. Seeing that the noise is affected by voxel size (Figure 1), a correction factor was required to allow for the comparison of CNRs from images with different voxel sizes, resulting in the following equation:

$$CNR_{AIR} = \frac{MGV_{PMMA} - MGV_{AIR}}{\sqrt{(SD_{PMMA}.Voxel^{0.608})^2 + (SD_{AIR}.Voxel^{0.608})^2}}$$

with MGV, the mean grey value; SD, the standard deviation; and Voxel, the voxel size (millimetre) of the image. The correction factor for voxel size was determined by scanning the PMMA phantom with 17.5, 87.5 and 175 mAs using 3D Accuitomo 170 and reconstructing the raw data at varying voxel sizes (0.08, 0.125, 0.16, 0.2, 0.25 and 0.3 mm). For each mAs setting, the SD of grey values (*i.e.* noise) was determined as a function of voxel size and fitted using an equation with the formula $y = a\,x^{-b}$. The correction factor for voxel size was then determined as the average of the $-b$ values for the three mAs settings (Figure 1). It should be noted that no correction for the grey value range (*i.e.* effective bit depth) was needed, as the CNR calculation itself takes the grey value range into account.

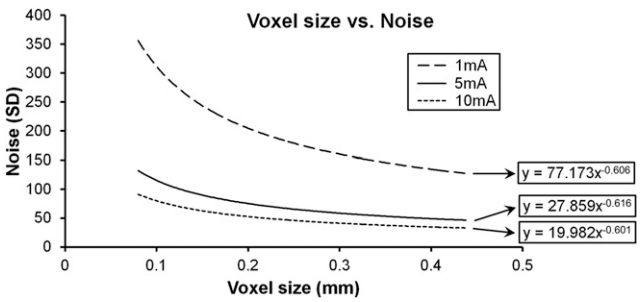

Figure 1 Determination of correction factor for voxel size. Noise was plotted *vs* voxel size for scans acquired at 3 mA settings of the 3D Accuitomo® 170 (J. Morita Manufacturing Corporation, Kyoto, Japan). Exposure time was fixed at 17.5 s. After fitting the data to the equation $y = a\,x^{-b}$, the average value of $-b$ was 0.608.

Clinical image quality

An anthropomorphic skull phantom (RANDO®; The Phantom Laboratory, Salem, NY) was used (Figure 2). The phantom represents an adult male (175 cm tall; 73.5 kg) and consists of a human skull with full dentition, embedded in a soft-tissue-equivalent material (*i.e.* polyurethane) simulating the muscle tissue with randomly distributed fat. CBCT scanning was performed using the range of exposure settings shown in Table 1. For each of the 47 CBCT data sets, 8 axial slices and 1 coronal slice with relevant anatomical landmarks were selected and combined in a stack.

Six experienced dentomaxillofacial radiologists were selected as observers. All observations were performed in a dimmed room, using a 20-inch medical display (MDRC-2120; Barco, Kortrijk, Belgium). Using ImageJ, images for each of the exposure protocols in Table 1 are shown. This was performed in a grouped, pairwise and stepwise manner, using the following approach (Figure 3):

- All images from a certain protocol were scored consecutively as one group. The CBCT model and scanning parameters were blinded, but the observers were aware that images from a certain group differed only in terms of mAs.

Figure 2 Anthropomorphic skull phantom (RANDO®; The Phantom Laboratory, Salem, NY), head and neck portion.

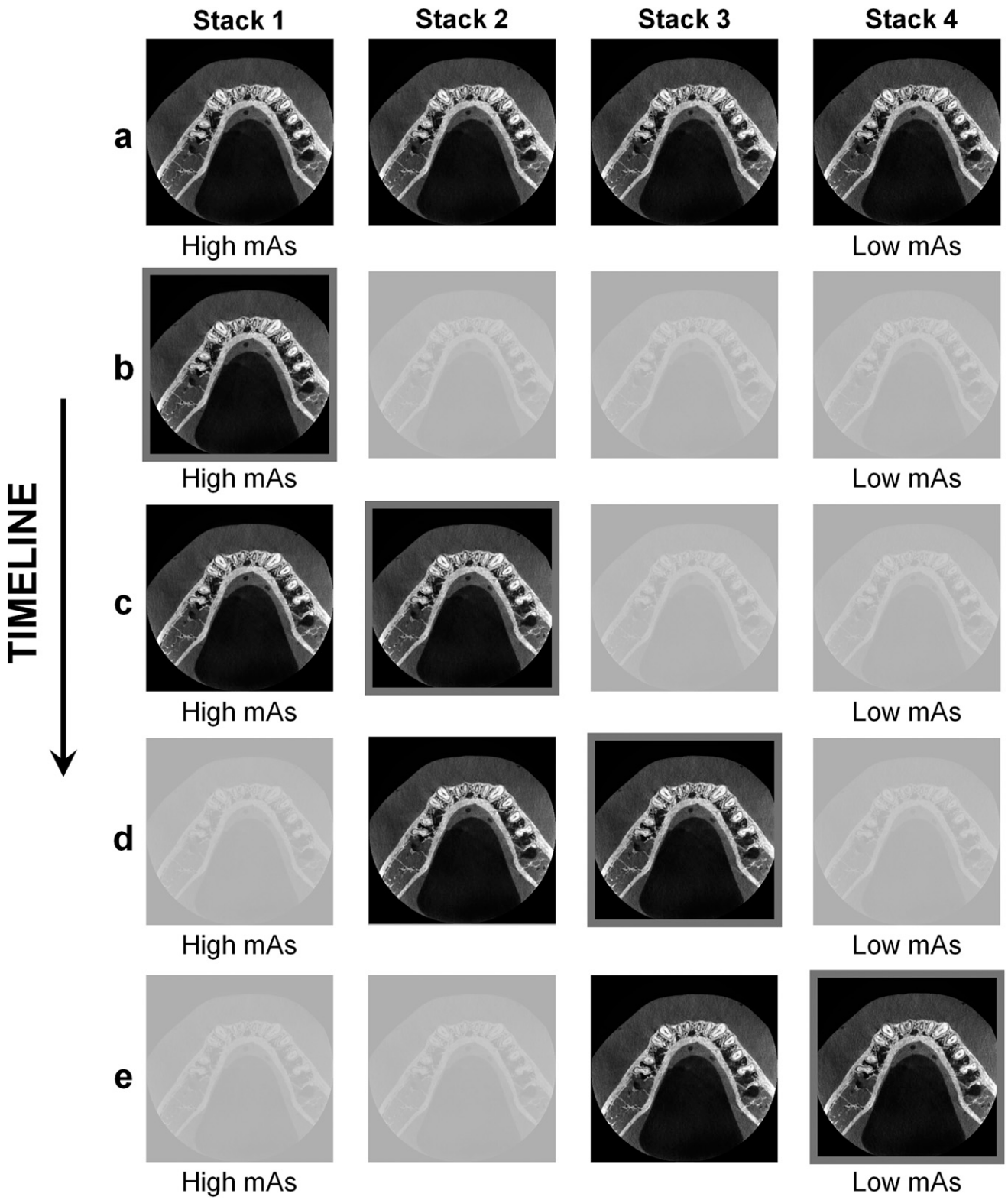

Figure 3 Workflow for observer study. Images being scored have a grey border. (a) All image stacks corresponding to one of the seven protocols in Table 1 were grouped and ordered according to their tube current–exposure time product (mAs) value. (b) Observers opened the stack with the highest mAs and provided scores. (c) The next image was opened and scored using the prior image as a reference. Scores provided for the reference image were either retained or lowered for the active image. (d) The reference image was closed, the active image became the new reference images, and the next image in the sequence was opened. (e) Steps (c–d) were repeated until the image with the lowest mAs was scored. The entire workflow is repeated for each protocol as shown in Table 1.

Table 2 Rating scale for observer study

Score	*Anatomical landmarks*	*Acceptability for clinical application*
1	Very poor visibility	Certainly not acceptable
2	Poor visibility	Probably not acceptable
3	Acceptable visibility	Probably acceptable
4	Excellent visibility	Certainly acceptable

- Images in each group were coded according to the mAs (*e.g.* "Stack 1" for the highest mAs up to "Stack 4" for the lowest mAs). The observers were instructed to open the image corresponding to the highest mAs first (*i.e.* "Stack 1") and to score the visibility of anatomical structures and clinical applicability using the parameters listed below.
- When finished scoring, the observers did not close the image but kept it open as a reference. They opened the next image in the group (*i.e.* "Stack 2"), compared it with the prior image for each scoring criterion and decided whether any of the scores provided for the "reference" image should be lowered for the "active" image. Increasing the scores was not allowed; only an identical or lower score than the prior image was possible. After scoring, the reference image was closed, the active image became the new reference image and the next image in the group was opened. This was repeated until all images in the group were scored.
- This procedure was repeated for each of the seven groups of images.

The observers were allowed to adjust brightness and contrast, and instructed to fine-tune grey level display for optimal visualization of the different anatomical landmarks, rather than using a single window/level setting for the entire evaluation. The general impression regarding the visibility (*i.e.* contrast and detail) of the ten different anatomical structures was scored: mandibular symphysis, mental foramen, cortical bone, lamina dura, periodontal ligament (PDL) space, pulp canal, enamel, maxillary suture, maxillary incisive foramen and trabecular bone. The observers were instructed to evaluate each structure in the entire image, rather than focus on a specific region. For all structures that were present in both jaws (*i.e.* cortical bone, lamina dura, PDL space, pulp canal, trabecular bone), a separate score for upper and lower jaw was provided. In addition, the observers provided a score expressing the acceptability (*i.e.* diagnostic confidence) of the image for three clinical applications: dental implant planning, identification of root pathology (*e.g.* root fracture, not pathology surrounding the roots such as periapical cysts) and identification of sinus pathology. For all evaluations, a four-point rating scale was used, summarized in Table 2. Interobserver agreement was estimated using a weighted kappa, calculated with MedCalc v. 11.2 (MedCalc Inc., Mariakerke, Belgium).

The relationship between mAs, CNR_{AIR} and observer scores was evaluated. Two approaches were used to determine preliminary minimally acceptable values for mAs and CNR_{AIR}. The first was based on a threshold of 2.5 for observer scoring, being the limit between acceptable and unacceptable image quality. For each of the seven exposure protocols in Table 1, the minimal mAs at which average observer scores were >2.5 was derived for each of the three selected clinical applications. The CNR corresponding to that particular mAs value was considered as the first minimally acceptable value. A second minimally acceptable value was determined as the CNR corresponding to the mAs for which all observers scored the image 3 or more.

Results

Scatter plots for CNR *vs* mAs are provided in Figure 4. For 3D Accuitomo 170, a clear hyperbolic relationship was seen, with CNR decreasing considerably at very low mAs levels and barely increasing at very high mAs levels. For the other devices, either a curved or linear section of a hyperbolic relationship was found.

Selected axial slices for each exposure protocols at the level of the mental foramen and maxillary bone are

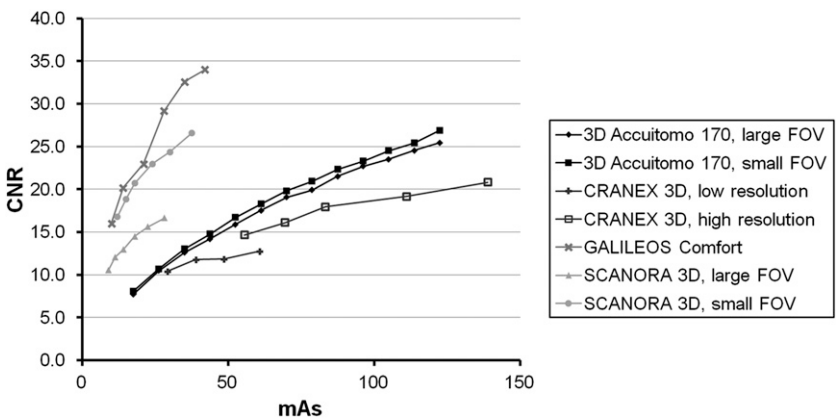

Figure 4 Contrast-to-noise ratio (CNR) *vs* tube current–exposure time product (mAs) for all protocols. 3D, three dimensional; FOV, field of view. CRANEX® 3D and SCANORA® 3D (Soredex, Tuusula, Finland); GALILEOS® Comfort (Sirona Dental Systems Gmbh, Bensheim, Germany); and 3D Accuitomo® 170 (J. Morita Manufacturing Corporation, Kyoto, Japan).

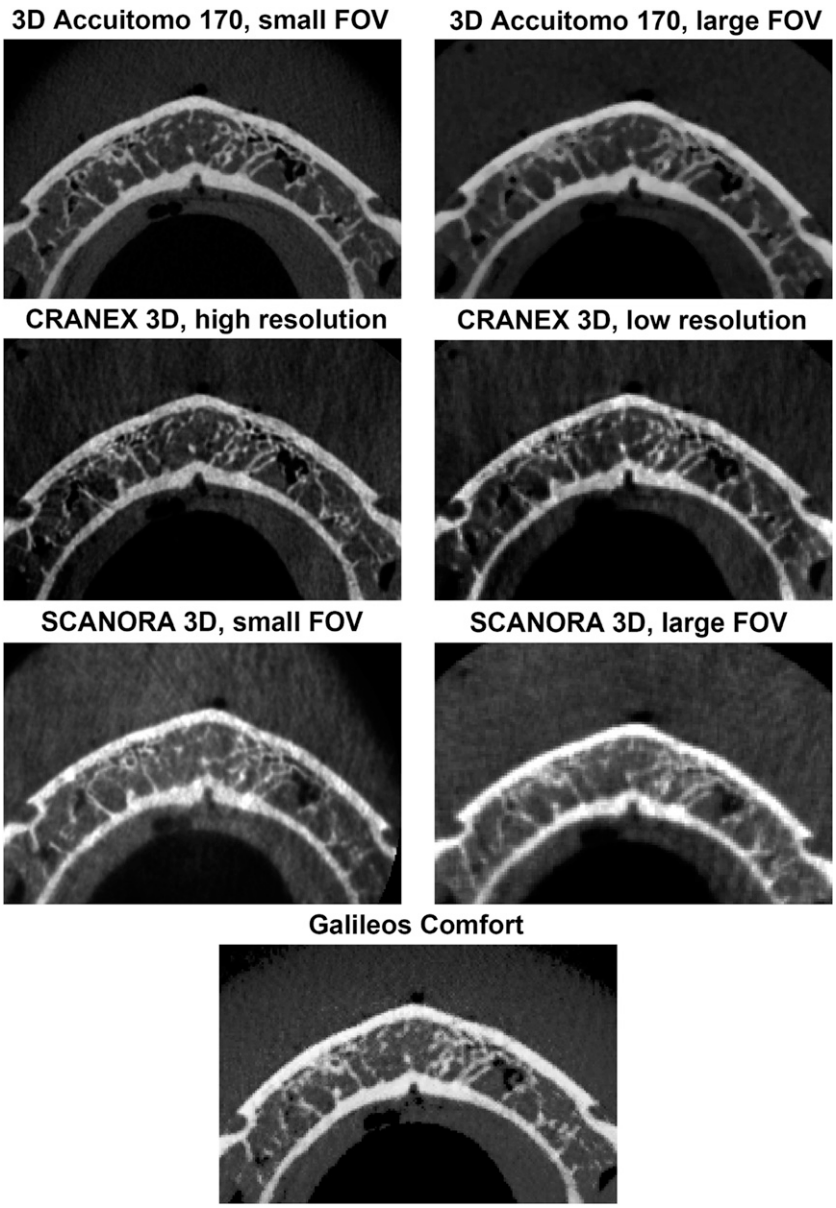

Figure 5 Axial slices at the level of the mental foramen, using the default tube current–exposure time product for each imaging protocol. Images were cropped and enlarged, and are for illustration purposes only. 3D, three dimensional; FOV, field of view. CRANEX® 3D and SCANORA® 3D (Soredex, Tuusula, Finland); GALILEOS® Comfort (Sirona Dental Systems Gmbh, Bensheim, Germany); and 3D Accuitomo® 170 (J. Morita Manufacturing Corporation, Kyoto, Japan).

shown in Figures 5 and 6, respectively. For each protocol, the default mAs for adult male patients was selected for these figures.

Kappa values representing interobserver agreement were between 0.34 and 0.68 with an average of 0.47 (Table 3). Out of 15 pairwise comparisons between observers, 8 were in the 0.4–0.6 (moderate agreement) range and 2 in the 0.6–0.8 (substantial agreement) range.

Figure 7 demonstrates the relationship between the CNR and the average observer score for all parameters. To calculate this average, values for mandible and maxilla (*e.g.* for cortical bone) were first averaged before calculating the overall mean value. Considering a score of 2.5 as the threshold value between an acceptable or unacceptable image (Table 2), most exposure protocols show an acceptable average score, even for the lowest mAs setting. Two exposure protocols dropped below this threshold for lower mAs values owing to low scores for the mandibular symphysis, PDL space and lamina dura.

Figure 8 shows the relationship between CNR and observer scores for the anatomical structures with the highest and lowest mean observer score. The highest score for all anatomical structures was for the mental foramen, for which all scores were three or higher (Figure 8). The maxillary lamina dura had the lowest score for all parameters, with all protocols reaching

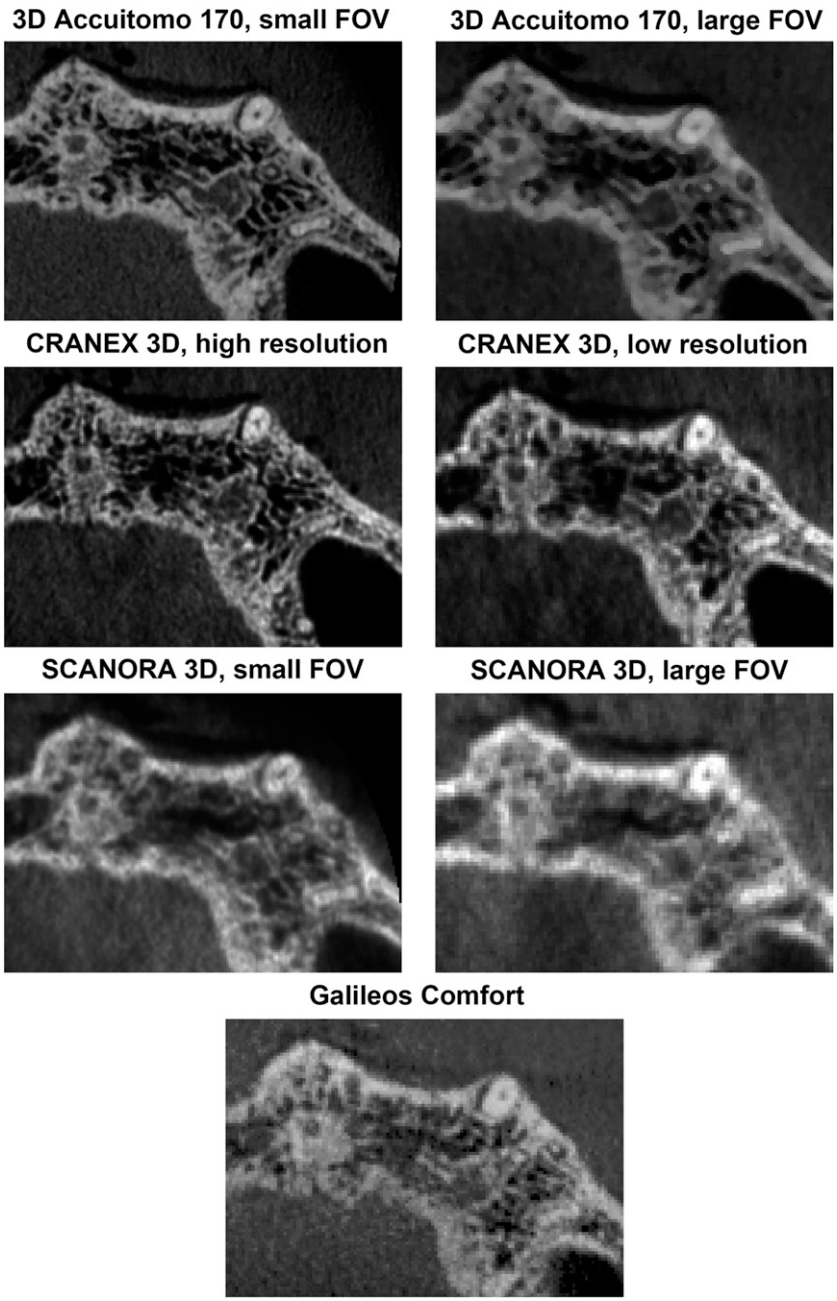

Figure 6 Axial slices at the level of the maxillary bone and sinus, using the default tube current–exposure time product for each imaging protocol. Images were cropped and enlarged, and are for illustration purposes only. 3D, three dimensional; FOV, field of view. CRANEX® 3D and SCANORA® 3D (Soredex, Tuusula, Finland); GALILEOS® Comfort (Sirona Dental Systems Gmbh, Bensheim, Germany); and 3D Accuitomo® 170 (J. Morita Manufacturing Corporation, Kyoto, Japan).

scores of two or lower at decreasing mAs levels (Figure 8). Differences between scores for maxilla and mandible were the highest for the cortical bone, for which the maxilla received a lower score (Figure 9). The difference between scores for maxilla and mandible were the largest for the GALILEOS Comfort, which showed higher mandibular scores for cortical and trabecular bone, in particular, and the lowest for the 3D Accuitomo 170, small FOV protocol, for which scores were almost identical (Table 4).

Figure 10 shows the observers' scores for the three clinical indications. Similar to the anatomical landmarks, a score of 2.5 corresponds to the threshold between an image that was deemed (on average) as being suitable for the given clinical indication, and one that was not.

Table 5 shows observer scores for all anatomical structures. For all seven exposure protocols, the minimum and maximum scores (*i.e.* scores for the lowest and highest mAs, respectively) for the 15 anatomical landmarks are provided. Table 6 contains the default

Table 3 Interobserver agreement (weighted kappa)

Observer	*Observer 2*	*Observer 3*	*Observer 4*	*Observer 5*	*Observer 6*
Observer 1	0.68	0.59	0.42	0.35	0.45
Observer 2		0.59	0.39	0.34	0.39
Observer 3			0.41	0.36	0.42
Observer 4				0.63	0.52
Observer 5					0.50

mAs for adult male patients for each exposure protocol, the minimal mAs level for which the scores for the three clinical indications was above the 2.5 threshold, and the corresponding CNR as a first minimally acceptable value. Also included in Table 6 is the minimal mAs value for which the score was three or more for each observer for the three clinical indications, and the corresponding CNR as a second minimally acceptable value. For three imaging protocols, there was no mAs value for which all observers scored the images three or more for any of the clinical applications. For another protocol, this was the case for "implant planning". For the two acceptability criteria (*i.e.* average score >2.5 or all observers scoring minimum 3), a wide range was seen for the minimal mAs value. For certain protocols, the lowest selectable mAs value was considered acceptable by all six observers. For several protocols, minimally acceptable mAs values were considerably below the default values for adult male patients, with possible mAs reductions of ≥50% found in a number of cases. A similar range as that of the minimal mAs values is seen for the corresponding CNR values. Particularly high CNR values corresponding to a minimally acceptable clinical image quality were found for the GALILEOS Comfort and SCANORA 3D, large FOV.

Discussion

The main objective of this study was to investigate the effect of mAs (*i.e.* radiation dose) reduction on CNR and clinical image quality in CBCT. In current clinical practice, the choice of exposure levels is still partly manufacturer-driven and partly determined by the personal experience of the CBCT user. The manufacturer always provides the user with one or more default exposure protocols. In addition, as the user gathers experience with the selectable exposure levels, he can fine-tune exposures for different patient groups. This study found that, in many cases, the mAs can be lowered considerably compared with the default setting while keeping image quality acceptable. The visualization of relatively large, high-contrast structures such as the cortical bone can be performed at a lower dose than that of small or low-contrast structures such as the lamina dura and PDL space. Similarly, mAs can be lowered for clinical applications with relatively low image quality requirements (*e.g.* implant planning) compared with those requiring high detail (*e.g.* root pathology).

A few considerations need to be made when interpreting the clinical relevance of these findings. Although the anthropomorphic phantom used in this study contains a real adult male skeleton with teeth and complete soft-tissue simulation, image quality based on its images may overestimate actual clinical image quality somewhat. Owing to the relatively long scan time in CBCT (typically 15–20 s, but as short as 5 s or as long as 40 s), image quality is affected by patient motion even when proper fixation is used, leading to slight blurring or more severe artefacts.[20] Also, metal objects such as restorations and implants lead to artefacts that can

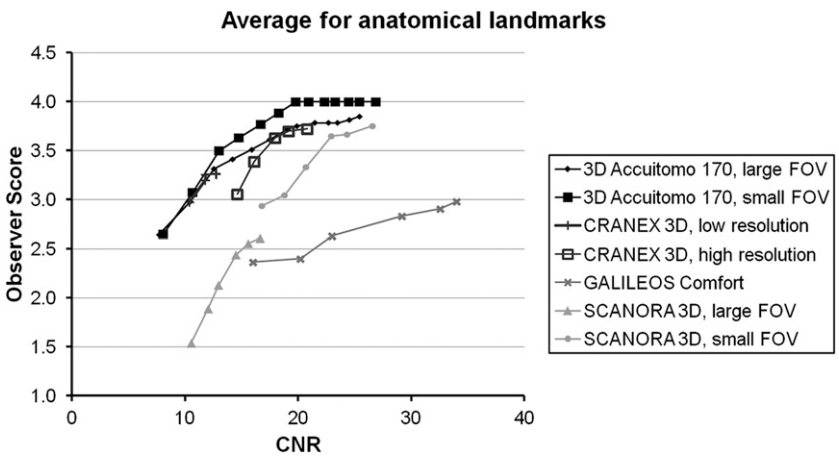

Figure 7 Relationship between contrast-to-noise ratio (CNR) and average observer score for all anatomical landmarks. 3D, three dimensional; FOV, field of view. CRANEX® 3D and SCANORA® 3D (Soredex, Tuusula, Finland); GALILEOS® Comfort (Sirona Dental Systems Gmbh, Bensheim, Germany); and 3D Accuitomo® 170 (J. Morita Manufacturing Corporation, Kyoto, Japan).

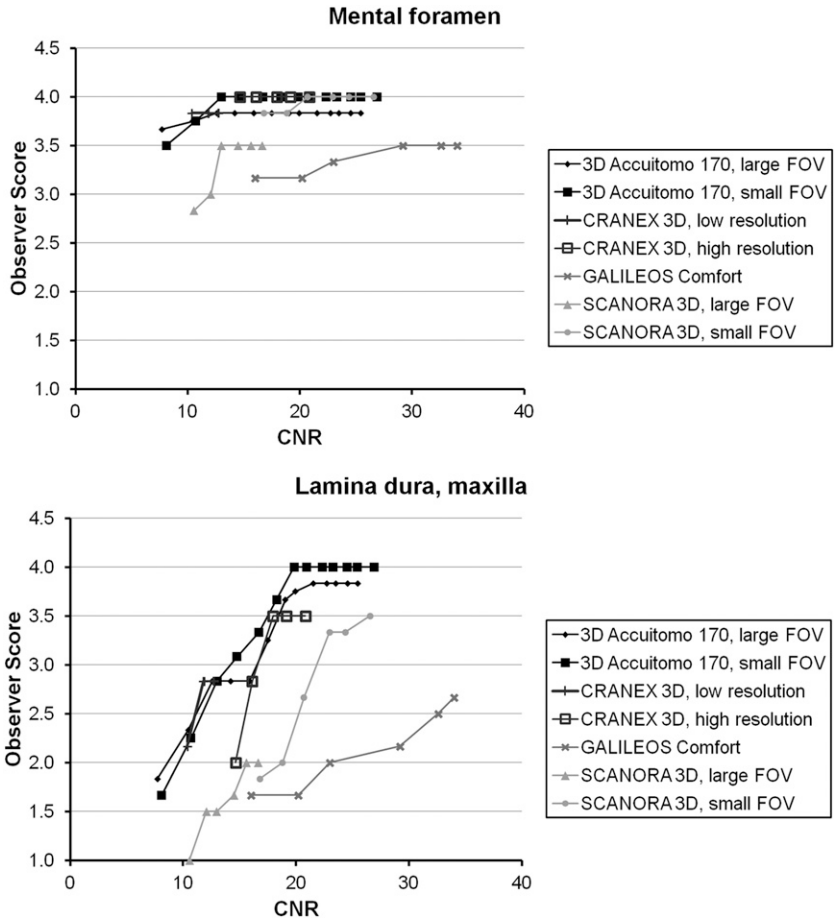

Figure 8 Relationship between contrast-to-noise ratio (CNR) and observer score for mental foramen and maxillary lamina dura. 3D, three dimensional; FOV, field of view. CRANEX® 3D and SCANORA® 3D (Soredex, Tuusula, Finland); GALILEOS® Comfort (Sirona Dental Systems Gmbh, Bensheim, Germany); and 3D Accuitomo® 170 (J. Morita Manufacturing Corporation, Kyoto, Japan).

extend throughout the FOV, although it should be noted that these artefacts are not or hardly affected by the mAs.[21] Regardless, the current results indicate that efforts should be taken to follow the as low as reasonably achievable principle in CBCT by minimizing mAs instead of relying on a default setting.

The evaluation of clinical image quality is prone to subjectivity. In this study, on average, scores between observers differed approximately 40% of the time. On the other hand, technical image quality parameters can be clearly defined and measured in an objective, standardized way; however, they cannot be closely linked to clinical image quality. CNR was selected as a technical image quality parameter for this study, as it can be measured in a straightforward fashion, shows a distinct relationship with tube output (mAs) and can be directly interpreted.[22,23] Although both CNR and clinical image quality were affected by mAs, the relationship between CNR and clinical image quality was specific for each CBCT model, and even differed between exposure protocols from the same model. Although the tube voltage (kV) was similar for all CBCTs (85–90 kV), varieties in the ratio between CNR and mAs could be caused by an interplay between other exposure factors (*e.g.* tube filtration, FOV size), the efficiency of the detector and reconstruction-related factors (*e.g.* filtering, voxel size).

The relationship between CNR and observer scores was reasonably consistent between 3D Accuitomo 170 and CRANEX 3D. For SCANORA 3D and GALILEOS Comfort, observer scores were low relative to CNR. The most important factor that caused this discrepancy is spatial resolution. As revealed in a *post hoc* discussion with the observers, lower scores for these devices were primarily caused by an inferior sharpness compared with the other protocols. CNR calculation did take spatial resolution into account to some extent, by correcting noise values in function of the voxel size. However, as demonstrated by Pauwels et al,[10] the voxel size does not always reflect the actual spatial resolution of an image. This is confirmed in the present study, as the two protocols of the 3D Accuitomo 170 received similar scores despite a two-fold difference in voxel size. A similar finding was seen for the CRANEX 3D. It is clear that the definition of standardized objective image quality criteria for CBCT, with a stable relationship with clinical image

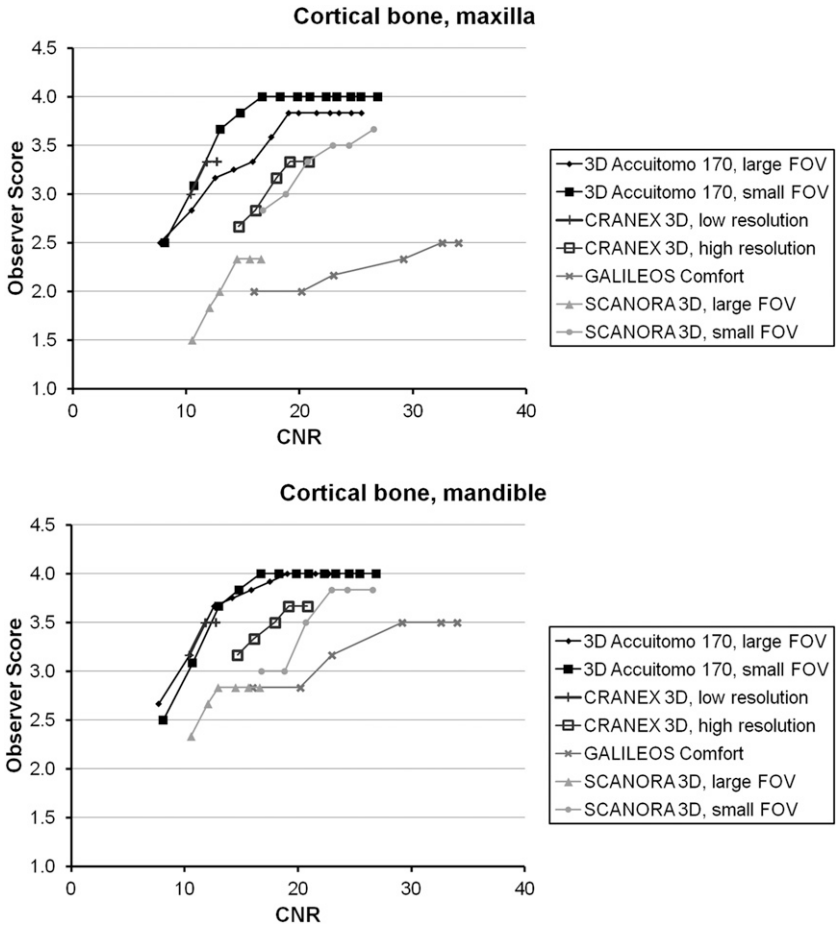

Figure 9 Relationship between contrast-to-noise ratio (CNR) and observer score for cortical bone, maxilla and mandible. 3D, three dimensional; FOV, field of view. CRANEX® 3D and SCANORA® 3D (Soredex, Tuusula, Finland); GALILEOS® Comfort (Sirona Dental Systems Gmbh, Bensheim, Germany); and 3D Accuitomo® 170 (J. Morita Manufacturing Corporation, Kyoto, Japan).

quality over varying exposure protocols and CBCT models, remains a challenge.

The current results allow for the definition of preliminary minimally acceptable values for CNR_{AIR}, which can be used as a starting point for future investigations. A strong point to be made is that these minimally acceptable values should not be confused with diagnostic reference levels, which indicate a level of patient dose that can be achieved for a given imaging technique in a certain geographical region.[24] The use of reference levels based on image quality should not be carried out in a radiation protection context, as the intention of "reaching" a certain image quality does not correspond with the principles of as low as reasonably achievable and diagnostic reference levels. Instead, they should be used only to indicate a potential image quality concern during research and development, acceptance testing or quality control. If

Table 4 Difference between mandibular and maxillary scores. Positive values denote a higher score for mandible

CBCT device and protocol	*Cortical bone*	*Trabecular bone*	*Periodontal ligament space*	*Lamina dura*	*Pulp canal*
3D Accuitomo 170, large FOV	0.27	−0.15	−0.01	0.07	0
3D Accuitomo 170, small FOV	0	0.04	0	0	0
CRANEX 3D, low resolution	0.05	0.05	0	0.03	0.01
CRANEX 3D, high resolution	0.15	0.03	0.00	0	0.09
GALILEOS Comfort	0.45	0.18	0.08	0.08	0
SCANORA 3D, large FOV	0.31	0.06	0.01	0.01	0
SCANORA 3D, small FOV	0.09	0.10	0.03	0.03	0
Average	0.19	0.04	0.02	0.03	0.01

FOV, field of view.
CRANEX® 3D and SCANORA® 3D obtained were from Soredex, Tuusula, Finland, GALILEOS® Comfort was obtained from Sirona Dental Systems Gmbh, Bensheim, Germany and 3D Accuitomo® 170 was obtained from J. Morita Manufacturing Corporation, Kyoto, Japan.

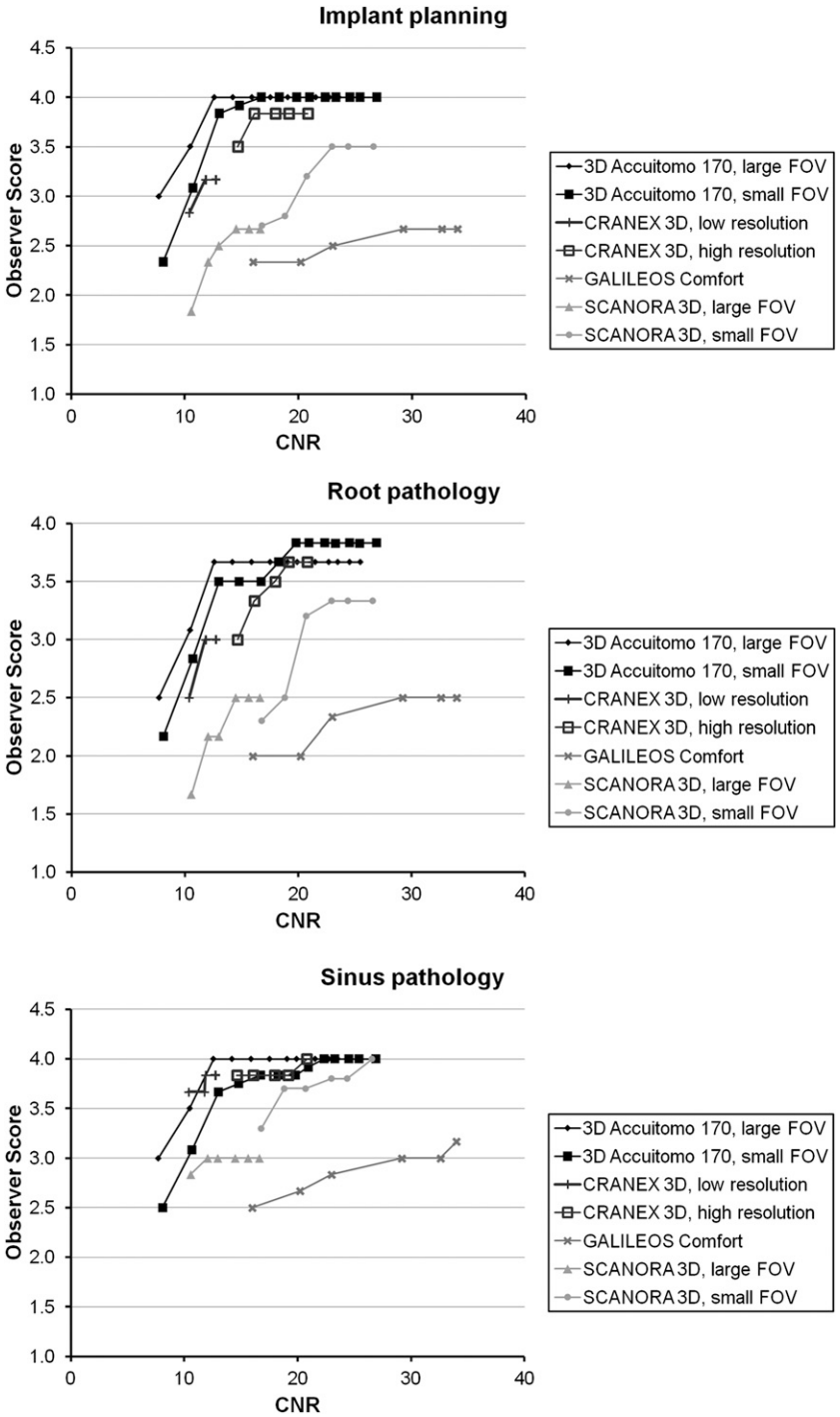

Figure 10 Contrast-to-noise ratio (CNR) *vs* observer scores for three clinical indications. 3D, three dimensional; FOV, field of view. CRANEX® 3D and SCANORA® 3D (Soredex, Tuusula, Finland); GALILEOS® Comfort (Sirona Dental Systems Gmbh, Bensheim, Germany); and 3D Accuitomo® 170 (J. Morita Manufacturing Corporation, Kyoto, Japan).

image quality is below a minimally acceptable value, more confirmation using (prior) patient images or anthropomorphic test objects is needed, and an investigation on possible causes for image quality aberrations should be conducted. If poor image quality is confirmed but the machine is found to be in working order, the cause is likely to be underexposure; only then can it be decided to increase mAs for future scans.

The CNR minimally acceptable values in Table 6 depended on clinical indication, although they did not always differ between implant planning, sinus pathology and root pathology. The CNR value

Table 5 Observer scores for anatomical structures

	Mandibular symphisis		*Mental foramen*		*Cortical bone, M*		*Cortical bone, m*		*Trabecular bone, M*		*Trabecular bone, m*		*Pulp canal, M*		*Pulp canal, m*	
CBCT device and protocol	*Min.*	*Max.*	*Min.*	*Max.*	*Min.*	*Max.*	*Min.*	*Max.*	*Min.*	*Max.*	*Min.*	*Max.*	*Min.*	*Max.*	*Min.*	*Max.*
3D Accuitomo 170, large FOV	2.8	3.8	3.7	3.8	2.5	3.8	2.7	4.0	2.5	4.0	2.5	3.8	2.5	3.8	2.5	3.8
3D Accuitomo 170, small FOV	3.2	4.0	3.5	4.0	2.5	4.0	2.5	4.0	1.8	4.0	2.2	4.0	2.5	4.0	2.5	4.0
CRANEX 3D, low resolution	2.2	2.5	3.8	3.8	3.0	3.3	3.2	3.5	3.0	3.2	3.2	3.3	3.0	3.2	3.2	3.2
CRANEX 3D, high resolution	3.2	3.7	4.0	4.0	2.7	3.3	3.2	3.7	3.0	3.8	3.2	3.8	3.2	3.5	3.3	3.7
GALILEOS Comfort	1.7	2.2	3.2	3.5	2.0	2.5	2.8	3.5	2.0	2.3	2.2	3.0	2.3	3.2	2.3	3.2
SCANORA 3D, large FOV	1.3	2.2	2.8	3.5	1.5	2.3	2.3	2.8	1.3	2.5	1.7	2.5	1.5	2.7	1.5	2.7
SCANORA 3D, small FOV	3.5	4.0	3.8	4.0	2.8	3.7	3.0	3.8	2.5	3.3	2.7	3.5	2.8	3.7	2.8	3.7

	Enamel		*Maxillary suture*		*Incisive foramen*		*PDL space, M*		*PDL space, m*		*Lamina dura, M*		*Lamina dura, m*	
CBCT device and protocol	*Min.*	*Max.*	*Min.*	*Max.*	*Min.*	*Max.*	*Min.*	*Max.*	*Min.*	*Max.*	*Min.*	*Max.*	*Min.*	*Max.*
3D Accuitomo 170, large FOV	2.7	3.8	2.8	4.0	3.2	3.8	1.7	3.7	1.8	3.7	1.8	3.8	2.0	3.8
3D Accuitomo 170, small FOV	3.0	4.0	3.2	4.0	3.0	4.0	2.0	4.0	2.0	4.0	1.7	4.0	1.7	4.0
CRANEX 3D, low resolution	3.5	3.8	3.0	3.0	3.5	3.7	2.3	3.0	2.3	3.0	2.2	2.8	2.2	3.0
CRANEX 3D, high resolution	2.5	3.3	3.8	4.0	3.8	4.0	2.0	3.8	2.0	3.8	2.0	3.5	2.0	3.5
GALILEOS Comfort	2.5	2.8	3.0	3.7	2.8	3.5	1.8	2.5	2.0	2.7	1.7	2.7	1.8	2.8
SCANORA 3D, large FOV	1.2	2.7	1.0	3.0	1.8	2.8	1.2	2.2	1.3	2.2	1.0	2.0	1.2	2.0
SCANORA 3D, small FOV	2.5	3.8	3.7	4.0	3.7	4.0	1.8	3.3	2.0	3.3	1.8	3.5	2.0	3.5

M, maxilla; m, mandible; Min., minimum; Max., maximum; PDL, periodontal ligament.
CRANEX® 3D and SCANORA® 3D were obtained from Soredex, Tuusula, Finland, GALILEOS® Comfort was obtained from Sirona Dental Systems Gmbh, Bensheim, Germany and 3D Accuitomo® 170 was obtained from J. Morita Manufacturing Corporation, Kyoto, Japan.

corresponding to an observer score of ≥3 was usually higher than the CNR value corresponding to an average score >2.5, as the former criterion is more strict. For all CBCT devices combined, the lowest CNR values corresponding to an acceptable image quality for implant/root/sinus were 7.7 for the first criterion and 12.6/11.8/10.4 for the second, respectively. mAs corresponding to these values was 18 and 35/39/29, respectively. As seen from the GALILEOS Comfort and SCANORA 3D results in the present study, CNR values far above these thresholds do not necessarily imply that the exposure levels for these protocols can be lowered considerably; as it was shown that CNR can overestimate clinical image quality, the values proposed above can only be considered as "minimally acceptable values" as discussed in the paragraph above. It is not yet feasible to determine (maximal) values or ranges for CNR above which the exposure should be lowered.

In conclusion, although noise increased at a lower mAs, clinical image quality often remained acceptable at exposure levels below the manufacturer's recommended setting for certain patient groups. The definition of standardized objective image quality criteria for CBCT can guide all parties involved in CBCT imaging (*i.e.* users, manufacturers, medical physicists) to achieve minimal exposure levels in all circumstances. Currently, it is not possible to determine minimally acceptable levels for image quality that are applicable to multiple CBCT models.

Table 6 Minimally acceptable mAs and contrast-to-noise ratio (CNR) values according to two acceptability criteria, for three clinical indications (implant planning, root pathology and sinus pathology)

		Average scores >2.5						*All observers scored ≥3*					
		Implant		*Root*		*Sinus*		*Implant*		*Root*		*Sinus*	
CBCT	*Default mAs*[a]	*mAs*	*CNR*	*mAs*	*CNR*	*mAs*	*CNR*	*mAs*	*CNR*	*mAs*	*CNR*	*mAs*	*CNR*
3D Accuitomo 170 large FOV	87.5	18[b]	7.7	18[b]	7.7	18[b]	7.7	35	12.6	35	12.6	35	12.6
3D Accuitomo 170 small FOV	87.5	18[b]	7.7	26	10.7	18[b]	7.7	35	13.0	35	13.0	35	13.0
CRANEX 3D low resolution	48.5	29[b]	10.4	29[b]	10.4	29[b]	10.4	/	/	39	11.8	29[b]	10.4
CRANEX 3D high resolution	79.5	56[b]	14.6	56[b]	14.6	56[b]	14.6	70	16.1	69	16.1	56[b]	14.6
GALILEOS Comfort	28	21	23.0	28	29.2	10	16.0	/	/	/	/	/	/
SCANORA 3D large FOV	18	14	13.0	18	14.5	9[b]	10.6	/	/	/	/	/	/
SCANORA 3D small FOV	24	12[b]	16.8	15	18.8	12[b]	16.8	24	23.0	19	20.7	12[b]	16.8
Average		24	13.3	27	15.1	22	12.0	41	16.2	39	14.8	34	13.5
Standard deviation		15	5.5	14	7.2	16	3.8	20	4.8	18	3.7	16	2.4

mAs, tube current–exposure time product.
CRANEX® 3D and SCANORA® 3D were obtained from Soredex, Tuusula, Finland, GALILEOS® Comfort was obtained from Sirona Dental Systems Gmbh, Bensheim, Germany and 3D Accuitomo® 170 was obtained from J. Morita Manufacturing Corporation, Kyoto, Japan.
[a]For adult male patients.
[b]The lowest selectable mAs value for this protocol.

References

1. Pauwels R, Cockmartin L, Ivanauskaité D, Urbonienė A, Gavala S, Donta C, et al; SEDENTEXCT Project Consortium. Estimating cancer risk from dental cone-beam CT exposures based on skin dosimetry. *Phys Med Biol* 2014; **59**: 3877–91. doi: 10.1088/0031-9155/59/14/3877
2. ICRP. The 2007 Recommendations of the International Commission on Radiological Protection. ICRP Publication 103. *Ann ICRP* 2007; **37**: 1–332.
3. Nemtoi A, Czink C, Haba D, Gahleitner A. Cone beam CT: a current overview of devices. *Dentomaxillofac Radiol* 2013; **42**: 20120443. doi: 10.1259/dmfr.20120443
4. Pauwels R, Silkosessak O, Jacobs R, Bogaerts R, Bosmans H, Panmekiate S. A pragmatic approach to determine the optimal kVp in cone beam CT: balancing contrast-to-noise ratio and radiation dose. *Dentomaxillofac Radiol* 2014; **43**: 20140059. doi: 10.1259/dmfr.20140059
5. Liang X, Jacobs R, Hassan B, Li L, Pauwels R, Corpas L, et al. A comparative evaluation of cone beam computed tomography (CBCT) and multi-slice CT (MSCT) part I. On subjective image quality. *Eur J Radiol* 2010; **75**: 265–9. doi: 10.1016/j.ejrad.2009.03.042
6. Park YS, Ahn JS, Kwon HB, Lee SP. Current status of dental caries diagnosis using cone beam computed tomography. *Imaging Sci Dent* 2011; **41**: 43–51. doi: 10.5624/isd.2011.41.2.43
7. Esposito S, Cardaropoli M, Cotti E. A suggested technique for the application of the cone beam computed tomography periapical index. *Dentomaxillofac Radiol* 2011; **40**: 506–12. doi: 10.1259/dmfr/78881369
8. Liang X, Lambrichts I, Sun Y, Denis K, Hassan B, Li L, et al. A comparative evaluation of cone beam computed tomography (CBCT) and multi-slice CT (MSCT). Part II: on 3D model accuracy. *Eur J Radiol* 2010; **75**: 270–4. doi: 10.1016/j.ejrad.2009.04.016
9. Loubele M, Maes F, Schutyser F, Marchal G, Jacobs R, Suetens P. Assessment of bone segmentation quality of cone-beam CT *versus* multislice spiral CT: a pilot study. *Oral Surg Oral Med Oral Pathol Oral Radiol Endod* 2006; **102**: 225–34. doi: 10.1016/j.tripleo.2005.10.039
10. Pauwels R, Beinsberger J, Stamatakis H, Tsiklakis K, Walker A, Bosmans H, et al; SEDENTEXCT Project Consortium. Comparison of spatial and contrast resolution for cone-beam computed tomography scanners. *Oral Surg Oral Med Oral Pathol Oral Radiol* 2012; **114**: 127–35. doi: 10.1016/j.oooo.2012.01.020
11. Watanabe H, Honda E, Kurabayashi T. Modulation transfer function evaluation of cone beam computed tomography for dental use with the oversampling method. *Dentomaxillofac Radiol* 2010; **39**: 28–32. doi: 10.1259/dmfr/27069629
12. Vassileva J, Stoyanov D. Quality control and patient dosimetry in dental cone beam CT. *Radiat Prot Dosimetry* 2010; **139**: 310–12. doi: 10.1093/rpd/ncq011
13. Pauwels R, Stamatakis H, Manousaridis G, Walker A, Michielsen K, Bosmans H, et al; SEDENTEXCT Project Consortium. Development and applicability of a quality control phantom for dental cone-beam CT. *J Appl Clin Med Phys* 2011; **12**: 245–60. doi: 10.1120/jacmp.v12i4.3478
14. Oliveira ML, Freitas DQ, Ambrosano GM, Haiter-Neto F. Influence of exposure factors on the variability of CBCT voxel values: a phantom study. *Dentomaxillofac Radiol* 2014; **43**: 20140128. doi: 10.1259/dmfr.20140128
15. Jessen KA. The quality criteria concept: an introduction and overview. *Radiat Prot Dosimetry* 2001; **94**: 29–32. doi: 10.1093/oxfordjournals.rpd.a006474
16. Alqerban A, Jacobs R, Fieuws S, Willems G. Comparison of two cone beam computed tomographic systems *versus* panoramic imaging for localization of impacted maxillary canines and detection of root resorption. *Eur J Orthod* 2011; **33**: 93–102. doi: 10.1093/ejo/cjq034
17. Hashimoto K, Kawashima S, Kameoka S, Akiyama Y, Honjoya T, Ejima K, et al. Comparison of image validity between cone beam computed tomography for dental use and multidetector row helical computed tomography. *Dentomaxillofac Radiol* 2007; **36**: 465–71. doi: 10.1259/dmfr/22818643
18. Soğur E, Baksi BG, Gröndahl HG. Imaging of root canal fillings: a comparison of subjective image quality between limited cone-beam CT, storage phosphor and film radiography. *Int Endod J* 2007; **40**: 179–85. doi: 10.1111/j.1365-2591.2007.01204.x
19. Hashimoto K, Arai Y, Iwai K, Araki M, Kawashima S, Terakado M. A comparison of a new limited cone beam computed tomography machine for dental use with a multidetector row helical CT machine. *Oral Surg Oral Med Oral Pathol Oral Radiol Endod* 2003; **95**: 371–7. doi: 10.1067/moe.2003.120
20. Spin-Neto R, Mudrak J, Matzen LH, Christensen J, Gotfredsen E, Wenzel A. Cone beam CT image artefacts related to head motion simulated by a robot skull: visual characteristics and impact on image quality. *Dentomaxillofac Radiol* 2013; **42**: 32310645. doi: 10.1259/dmfr/32310645
21. Pauwels R, Stamatakis H, Bosmans H, Bogaerts R, Jacobs R, Horner K, et al; SEDENTEXCT Project Consortium. Quantification of metal artifacts on cone beam computed tomography images. *Clin Oral Implants Res* 2013; **24**(Suppl. A100): 94–9. doi: 10.1111/j.1600-0501.2011.02382.x
22. Funama Y, Sugaya Y, Miyazaki O, Utsunomiya D, Yamashita Y, Awai K. Automatic exposure control at MDCT based on the contrast-to-noise ratio: theoretical background and phantom study. *Phys Med* 2013; **29**: 39–47. doi: 10.1016/j.ejmp.2011.11.004
23. Muhogora WE, Devetti A, Padovani R, Msaki P, Bonutti F. Application of European protocol in the evaluation of contrast-to-noise ratio and mean glandular dose for two digital mammography systems. *Radiat Prot Dosimetry* 2008; **129**: 231–6. doi: 10.1093/rpd/ncn023
24. Vassileva J, Rehani M. Diagnostic reference levels. *AJR Am J Roentgenol* 2015; **204**: W1–3. doi: 10.2214/AJR.14.12794